

Individual Research Project Platform for Microrobot Navigation

Nafiseh Vahabi

Supervisors: Prof Guang-Zhong Yang, Dr Henry Ip and Dr Vincenzo Curto

February 28, 2014

1 Introduction

Magnetically actuated helical micromechanisms can be used in a variety of biomedical applications such as cell characterisation, targeted drug delivery and vivo diagnosis [7]. However, the extremely small size of the microrobots and the biofluid environment make the design aspect very challenging. The two main difficulties are the power source and finding suitable locomotion methods, as there are many cells, proteins and fibres in biofluids that prevent the motion of the microrobots. The common method of using an external magnetic field produced the most successful result [8].

2 Literature Review

The design of microrobots depends on their application and the desired task. The different microrobot designs are discussed in the following sections.

2.1 Microscrew Like Structure and Actuation Principle

2.1.1 Helical Shape

There are three common shapes of microrobots based on the rotary action; a helix, a screw and a twisted ribbon shape around its axis (Figure 1).

For the purpose of drilling into solid matter such as biological tissue the screw and helix design would be more appropriate. There is also the consideration of penetrating a solid material from a fluidic environment. In the fluidic regime the Reynold number (Re) has a substantial effect on a microdevice locomotion [7]. The Reynolds number describes the ratio of the inertial forces versus viscous forces according the following formula;

$$Re = \frac{UL\rho}{\mu} \quad (1)$$

Where U is velocity, L is characteristic length, ρ is the density and μ is viscosity of the fluid. In the case of the helical microdevice, the helical rotation will not move forward in the same way as in solid matter because whilst the device is rotating in a fluid environment, it only moves by a small percentage of its pitch length per rotation [7].

For the purposes of drug delivery the tabular and helical lipid microstructures were successful and both had a good loading capacity and propulsion efficiency. The rotational motion of helical micro swimmers is one of the most effective propulsion methods in the low Reynolds number scenarios because it leads to translational motion. Microrobots with the microspheres structure perform similarly to the helical swimmers and are capable of swimming in the flowing liquid within the microfluidic channel [3]. More recently, a three-dimensional porous micro-niches designed for cell transportation purposes used photocurable polymer for its fabrication method. To improve biocompatibility for in-vivo applications, the microrobot can be covered with a thin layer of titanium. In addition, the microrobot's structure was layered with nickel for the purpose of magnetic actuation. A magnetic manipulator rotates and translates the microrobot wirelessly. Most in-vivo environments are three-dimensional, hence the 3D navigation will be required for the successful microrobot [3]. Porous structures with the controllable porosity demonstrate improved characteristic such as high cell compactness and uniform cell distribution. Three-dimensional laser lithography is a state of the art technique to fabricate porous structures (Figure 3). In this method a building unit is a single ellipsoidal spot, which form as a result of concentration of two laser beams. A pre-programmed path is followed by controlling the movement of a piezoelectric stage precisely to partly expose the photoresist. After removing the unexposed photoresist a complete three-dimensional structure of the microrobot can be formed.

There are two main factors that affect the movements of the microrobot in the external magnetic field; low coercivity and high saturation magnetization. Also, the motion of the microrobot is related to its size given the same magnetic field and as such, by increasing the size of the microrobot with the inflexible magnetic material volume, the velocity will decrease [3]. The surface friction and the drag forces are two resistive forces that impede the microrobot's motion. Hence, the input magnetic force must be sufficient to overcome these forces for microrobot manipulation. Furthermore, the weight of the microrobot requires compensating gravity in the z-direction by the magnetic field. The navigation methodology

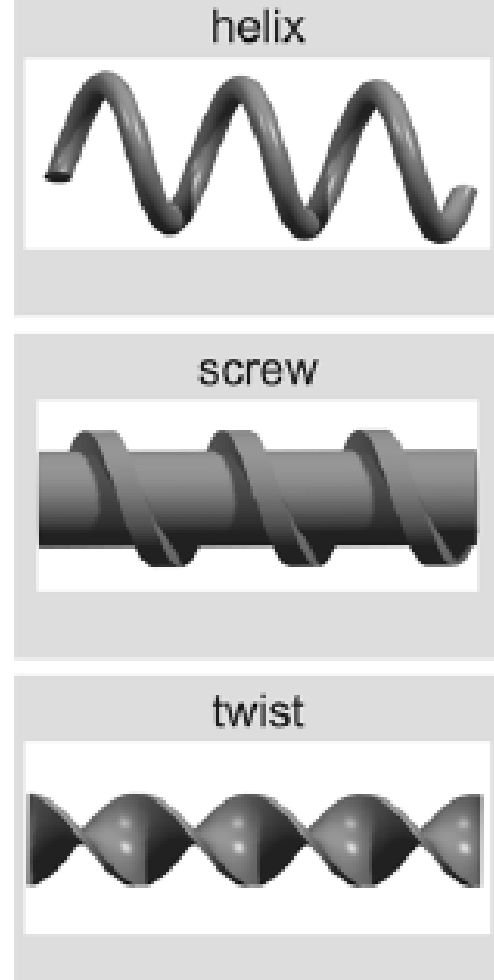


Figure 1: Three design of helical microswimmers. [7].

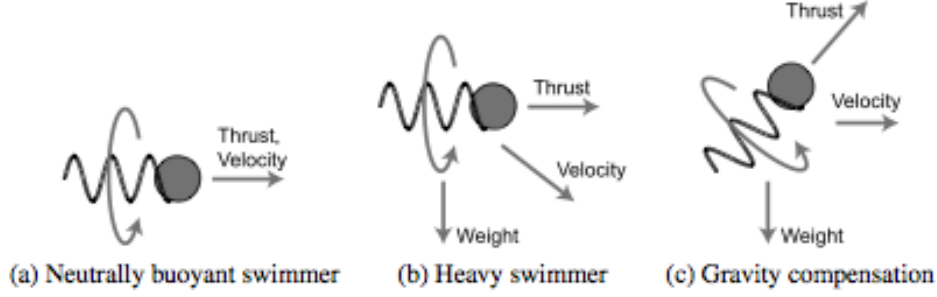


Figure 2: The effect of the gravity on the microrobot motion direction and gravity compensation [5].

should compensate for gravity to avoid sinking and enable velocity to be controlled wirelessly. Mahoney et al. described an algorithm for helical microswimmers velocity control plus gravity compensation. In the proposed model the correct pitch angle and rotation speed is calculated to achieve the commanded velocity [5].

The mathematic model below describes the microrobot translational movement;

$$\vec{F}_m + \vec{F}_r - \vec{F}_g = m(\vec{dv}/dt) \quad (2)$$

Where F_m , F_r and F_g are a magnetic force, overall resistive force and gravitational force respectively. M is a mass and v is a translational velocity of the microrobot [3].

The fabricated hexahedral microrobot and cylindrical microrobot can be seen in the Figure 3. For the fabrication method, because nickel is deposited uniformly on the surface of these microrobots, the Hexahedral structure has a greater amount of nickel deposited on its surface. Consequently, the magnetic force required for the hexahedral microrobot is greater than the cylindrical one while its translational velocity is lower than the cylindrical microrobots. Hence, the cylindrical structure is preferable for the purpose of minimising the resistive force against manipulation [3].

A magnetic field can be used for controlling teams of microrobots as well as a single one. Kim et al. proposed a method that used a combination of two magnetic materials to attain on/off magnetization of each microrobot. The overall control of the group of microrobots was achieved by managing the state of each agent. In addition, a second technique has been developed for

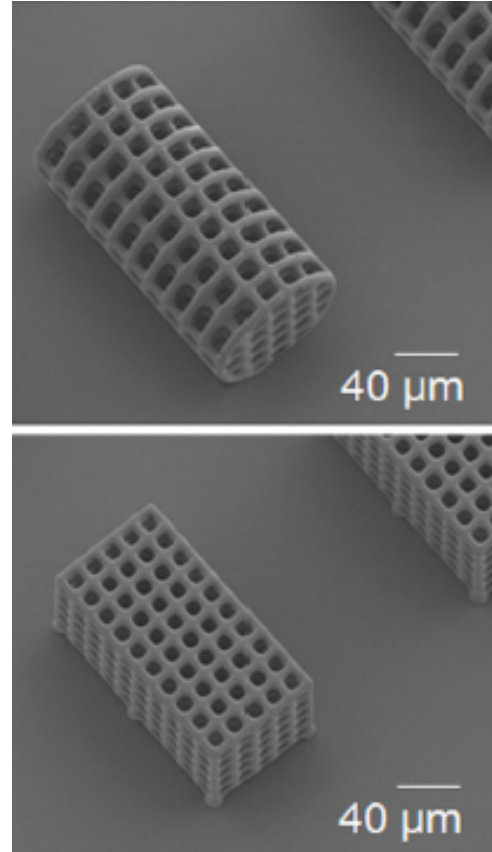


Figure 3: The image of two designs of fabricated microrobot under scan electron microscopy, cylindrical-shaped (first) and hexahedral-shaped (second) [3].

three-dimensional motion of the team of microrobots in a fluidic environment. In the latter method, each microrobot is designed in such a way that it uniquely responds to the same input magnetic field. Therefore, several microrobots can provide feedback position control in 3D system [3]. An untethered spherical magnetic micromanipulator creates a locally induced rotational fluid flow field. The created rotational flow propels micro-objects in the flow area. A team of microrobots could perform a complex task in micro-transport and micro-assembly [3].

In another study [11], a helical microrobot was designed to swim in a low Reynolds number fluid and a 3D direct laser writing method was applied as the preferable technique for fabrication. This fabrication method allows flexible design of microrobot in which two designs are selected to run the experiment. The first structure is a bare helical structure and the second one is the helical shape with the microholder attached at the end. Both designs will generate the corkscrew motion in a fluid environment when there is sufficient magnetic field. The second design (device with the microholder) is capable of transporting a microobject accurately to the target [11].

The fabrication process consists of the three stages that are fairly similar to the work performed by Kim et al.. In the first stage, direct laser writing in negative tone photoresist wrote the helical device. The developer then removed the unpolymerized photoresist. Finally, the developed helical swimmers were left for drying out and then coated in a thin layer of titanium and nickel for biocompatibility and magnetic actuation [11].

In Tottori et al. experiment eight different designs of microrobots were proposed and tested. The uniform static magnetic field was used to explore the magnetic shape anisotropy and the magnetic actuation was monitored in the rotating magnetic field. In the static magnetic field the set of microrobots had helical angles ranging from 45° to 70° when suspended in the deionised water.

This showed (Figure 4) that a smaller helix angle θ results in a less misalignment angle α because microrobots longest axes will be aligned to the direction of the external magnetic field. However in helical microrobot with larger helical angles, the magnetization direction would change to the radial axes of the helix [11]. In the rotating magnetic field, the micro helical swimmer exhibits different behaviours depending on the strength of the applied frequency in the fixed magnetic field. At low frequencies the micro helix oscillated around the helical axes, however by increasing the frequency the oscillating behaviour changed to the corkscrew motion. This is similar to characteristics of microrobots with an incorporated microholder [11].

The velocity of helical micro swimmers depends on their size and shape. A linear relationship was observed between the input frequencies and swimming velocity of the micro swimmers. The

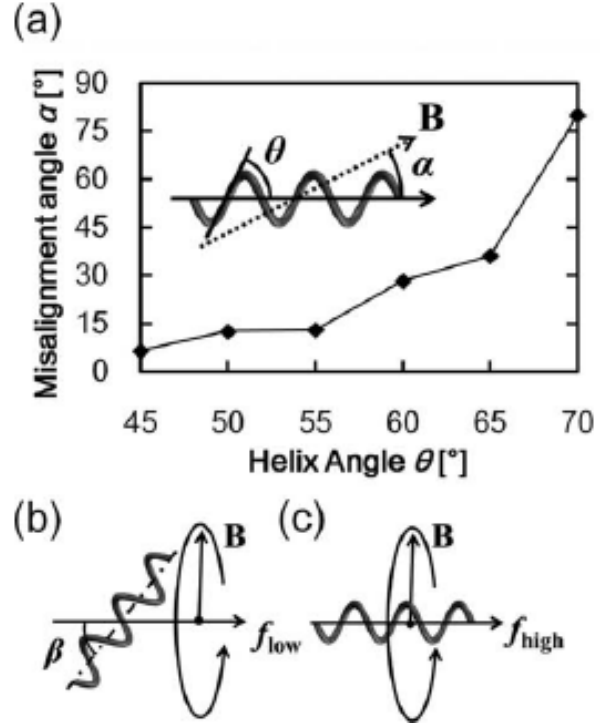


Figure 4: (a) The misalignment of helical angle α with different helix angle (b) the oscillation behaviour of the microswimmer with the high and low frequencies [11].

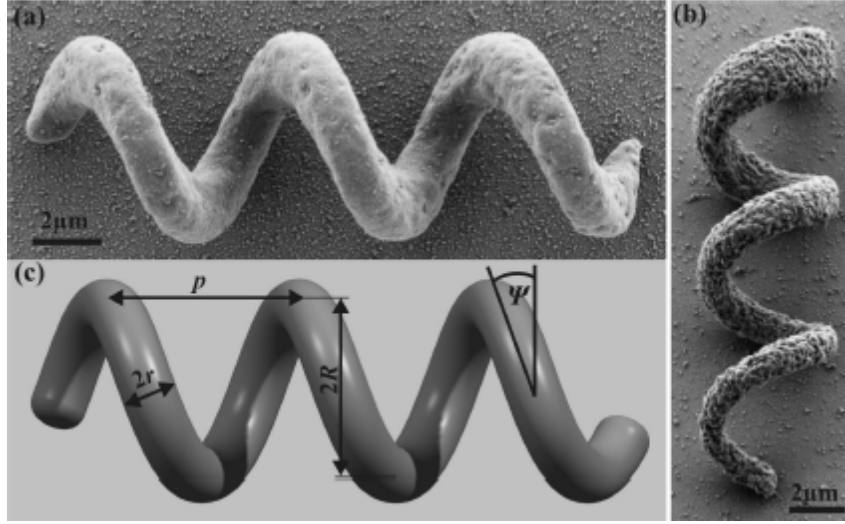


Figure 5: The prototype of microhelical device. (a) Scanning electron microscopic image of the micro polymer composite with the 2 vol.% nanoparticle fill factor and (b) 4 vol.% of nanoparticle fill factor. (c) The CAD model shows all the parameters required for the microhelical design [6].

outcome of the comparison between three microhelixes with the same helix angles showed that the microhelix with the greatest diameter has the highest speed, in accordance with the following formula;

$$U = \frac{(C_n - C_1) \sin \theta \cos \theta}{2(C_n \sin^2 \theta + C_1 \cos^2 \theta)} (d\varpi) \quad (3)$$

Where C_n is a drag coefficient perpendicular to the filament and C_1 is a drag coefficient parallel to the filament. ϖ is the rotational frequency and d is the rotational diameter of the helix [11].

The important role of helix angle in the magnetization structure of helical micro swimmers was confirmed by Peyer et al., who again used direct laser writing (DLW) as a fabrication method but applied (DLW) on the magnetic polymer composite (MPC). The MPC are non-cytotoxic and showed super paramagnetic characteristic because magnetic material was already included in the polymer.

The relationship between the torque T_d , the drag force F_d , the object's velocity U and rotational speed ω is linear and modelled by 6×6 resistant matrix as below;

$$\begin{bmatrix} F_d \\ T_d \end{bmatrix} = - \begin{bmatrix} A & B \\ B^T & C \end{bmatrix} \begin{bmatrix} U \\ \Omega \end{bmatrix}$$

Where A , B and C are matrices 3×3 and only depend on the object's geometry and fluid velocity. There are few methods in use to model the resistance matrices and low Reynolds flow such as the method of regularized stokeslets, the boundary element method and the method of fundamental solution. In designing a microrobot the main parameters required to concentrate on are the helicity angle ψ , the helix radius R , the pitch p and the filament radius r as illustrated in Figure 5 part (c).

Magnetic actuated microrobot is divided into two categories; torque driven microrobot and force driven microrobots. The micro robot using the torque-driven method is more favourable

than the force-driven method because their rotation is based on applying torque rather than a force to pull the device [6].

2.1.2 Helical Swimmer Fabrication

The fabrication of the microrobot was the main problem that recent fabrication methods offer a feasible solution for that [2]. The fabrication process consists of two stages. Initially the core structure of the artificial helical microswimmer is printed using 3D lithography and then electron beam evaporation is used for ferromagnetic thin film coating [10]. Performance of each microswimmer (with different design) can be scanned by the scanning electron microscope (SEM). After the fabrication process is completed, the next step is to release the structure into deionised water using the tungsten probe. The tank with deionised water is installed in the middle of the three-axis Helmholtz setup.

2.1.3 Tube Shape

Another approach for powering a micro robot is using the catalytic conversion of chemical energy into mechanical energy (Figure 6). In this method, the catalyst accelerates the consumption of hydrogen peroxide and helps the self-propulsion of micro robot to pump the fluid to transport cells and colloidal particles [13].

The catalytic tube (nanotube) is fabricated with a sub micrometer diameter. This technique is not applicable for the minimally invasive surgery (MIS) yet because the catalytic material used in the fabrication process of nanotubes is toxic and sustain viable mammalian cellular functions. Hence, biocompatible fuel is required to be developed in order to apply this technique in the live cell [13].

Alternatively, the micro driller can be powered and controlled by using an external magnetic field such that changes in the frequency of the rotating magnetic field switch the rotational orientation of the micro tool from the horizontal position to the vertical one. The vertical orientation of the rolled up microtube and its sharp helical design makes the device suitable for drilling into biological tissue. In addition, the micro driller can be used for targeted drug delivery in MIS [13].

2.2 Bioinspired Flagella (tail) Propulsion Microbots

One of the most challenging aspects of designing a robot on a very small scale such as a nanorobot is simplicity. The reason is, integration will become unfeasible on that scale if the design is complex. Hence the development of the nanorobot or even microrobot should be based on the essential functionality, avoiding any unnecessary components. Helical flagella and cilia are two well-known microswimmers in nature that have had their functionality employed for motion generation in artificial microrobots (Figure 7). Their motion generation mechanism relies on the drag

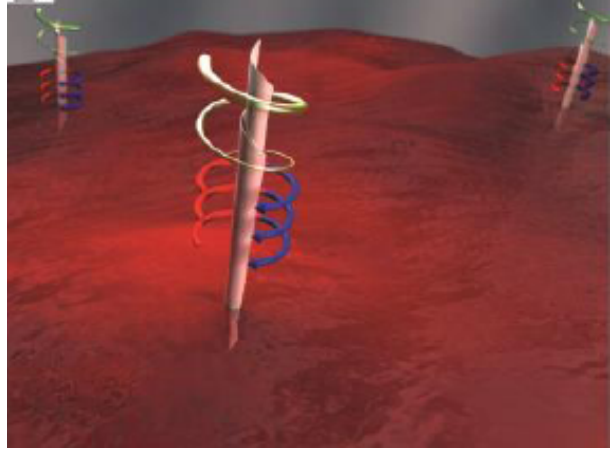


Figure 6: Demonstrating the drilling motion of the nanotubes under rotating magnetic field [13].

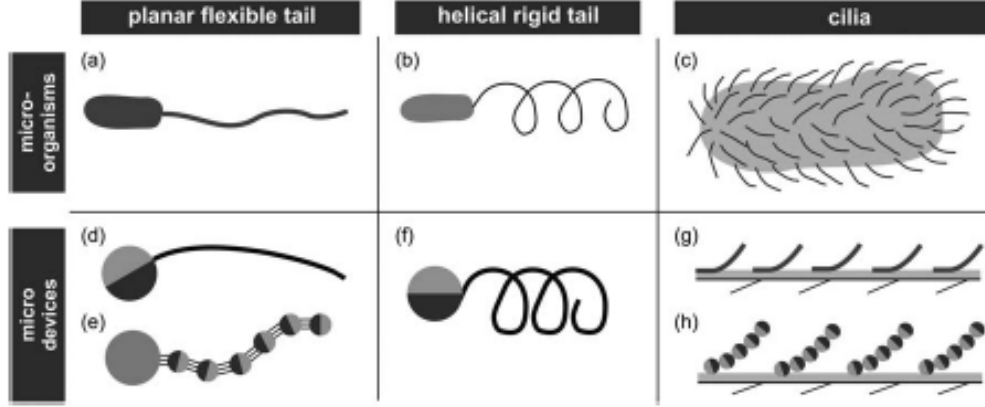


Figure 7: The illustration of both flagellum and cilia shapes and microdevices mimicked the flagellum and cilia structures. [8].

imbalance of a cylindrical element and non-reciprocal motion [2].

In 2007, Bell [2] presented the first artificial bacteria flagellum microrobots and then Zhang characterised them in 2009 [2]. This artificial microrobot was formed of two components; a rigid helical tail and a soft magnetic metal head. The head diameter was $2.8\mu m$ and its length was $30 - 100\mu m$. Since then, other scientists proposed a slightly different design structure, that all have the rigid helical tail structure. However, in some cases the magnetic materials is used in the device tail rather than the head [2]. The fabrication of the microrobot was the main problem that recent fabrication methods have now resolved by using DLW [2].

By learning from nature and mimicking the structure of live organisms, we can create successful scientific applications [9]. The helical rotation of flagella and the travelling wave beat of cilia are two non-reciprocal propulsion mechanisms in microorganisms. Mimicking a rotating flagellum at low Reynolds number to generate an adequate torque to overpower the high viscous drag requires two main elements; a rotary motor and a power source [9]. An electromagnetic rotary motor can be used in designing a helical flagella style microrobot that requires a considerable current. However piezoelectric rotary motors are an alternative option that are appropriate for miniaturisation but necessitate high input voltage. Hence, designing a microrobot with a combination of an onboard power source and a motor is a challenging task [9].

Another design of microswimmers was inspired by the function of magtigonemes in nature [10]. A smooth flagellum moves against the direction of the propagation of the flagella wave. However, the flagellum covered by magtigoneme propels in the same direction as the flagellum wave (Figure 8). Mimicking the structure of flagellum and using 3D lithography and electron beam evaporation formed the fabrication method in these microswimmers. The anisotropic

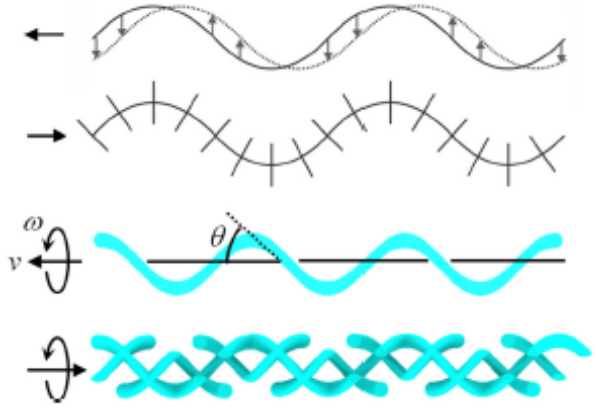


Figure 8: The structure of the smooth flagellum and a magtigonemes flagellum. [2].

viscous drag on flagella is an important fact for locomotion in low Reynolds number fluid. Flagella movement in the opposite direction of the flagella wave is because the viscous drag coefficient perpendicular to the flagella is greater than the viscous drag coefficient parallel to the flagella [10].

The rotating field, i.e. rotational frequency, field strength and angles that defined the rotational axis can be controlled by the current in the coil. The helical microrobots rotate synchronously with the rotation of the magnetic field and move forward and backward accordingly [10]. The displacement of the microswimmer along the rotational axis can be measured and the result used to calculate the average velocity of the swimmers. There is a linear relationship between an input field frequency and swimming speed. According to their result [10], a propulsive force generated by the mastigoneme is in opposite direction of the force generated by the main helical filament.

The swimming velocity of a mastigoneme helical swimmer is illustrated in (Figure 8) and can be estimated by the following symmetric propulsion matrix;

$$\begin{bmatrix} F \\ T \end{bmatrix} = \begin{bmatrix} A & B \\ B & C \end{bmatrix} \begin{bmatrix} \nu \\ \varpi \end{bmatrix}$$

The angular velocity is ϖ , velocity ν , external torque T and external force F . The propulsion matrix has two main components; one is for the main flagellum and the second is for the mastigonemes. After solving both part of the propulsion matrix, the velocity of the microswimmers is given by the equation below;

$$\nu = \frac{(B_1 + B_2)}{A_1 + A_2}(\omega) \quad (4)$$

Where

$$\begin{aligned} A &= A_1 + A_2 \\ B &= B_1 + B_2 \end{aligned} \quad (5)$$

However, this velocity is only valid if the external force is zero. The proposed design [10] is rigid and an external stimulus may be used to regulate the swimming speed and direction if the swimmer can fold and unfold their structure.

2.3 Plant-based Microbots

The helical microstructures are not limited to having flagellum-like structures and microbots with general cilia-like feature have been designed. Gao et al. observed the helical microstructures that imitates spiral water-conducting vessels of different plants.

The fabrication process involves coating isolated spiral xylem vessel plant fibres within a (Figure 5) thin magnetic layer. Xylem tissue transports the plant's required food such as water and other nutrition from the root to the leaves using capillary action [5]. Use of plant material in this method enables simple three-dimensional microswimmers fabrication and biocompatibility. In addition, the magnetic cover helps to ensure accurate directional control and high-speed propulsion. Therefore the fabrication processes were extremely simplified as the main component of the helical microswimmers is from nature and more than a million individual micro helicals can be made from a very small section of the plant stalk [5].

Using mechanical stretching can control geometric variables of the helical vessels such as the pitch and helix angle and hence plenty of helical microswimmers can be reproduced. The final shape of the helical microswimmer is determined mainly by the initial diameter of the unstretched spiral vessel. The process of stretching helical plant structure was performed via

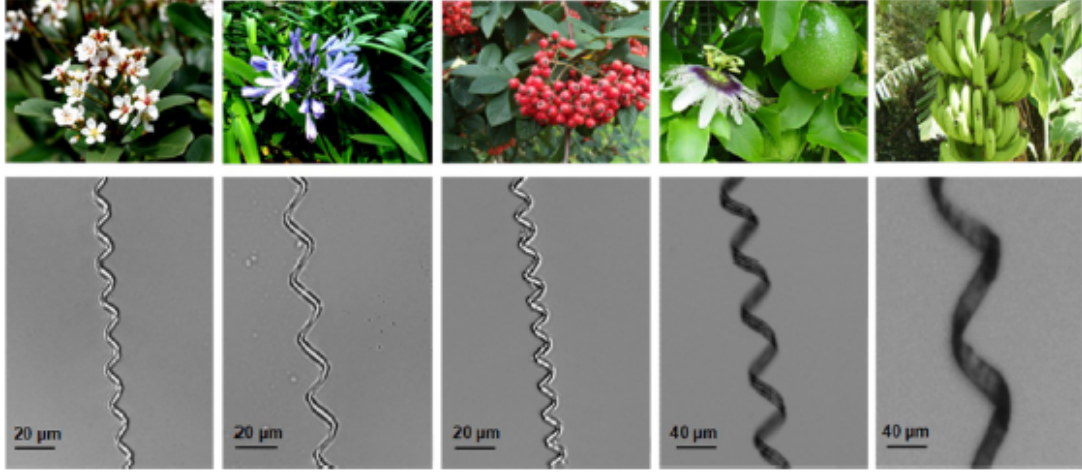


Figure 9: The shape of the Xylem in different plants . [5].

plastic deformation so that the number of helical turns are constant and tensile stretching of the plant fibre stretching is negligible [5].

The method used for precise propulsion control and characterising the locomotion behaviour of the plant-based microswimmers is similar to the method applied in Gao et al. study.

According to Gao et al. experiment, the plant-based microswimmers exhibited high speed movement in raw biological medium such as pure human serum under the rotating magnetic field. Moreover, the increased velocity of the biological fluid has a minor effect on the plant-driven microswimmers, which is an important advantage of this microdevice over the common microrobots.

2.4 Bioinspired Jellyfish

Jellyfish-like swimming robot is another robot design that scientists were interested in because of its unique swimming style. Different types of actuators are used to model jellyfish-like swimming robot such as shape memory alloy, ionic polymer metal composite. However, these jellyfish-like robots were unable to swim freely in three-dimensional space due to small propulsion force and were restricted due to the power supply wire. Therefore an external magnetic field was applied to compensate for this power wire issue [4].

3 Project Plan

For the purpose of this project different proposed structures of microrobots were studied and analysed. This will enable helical microswimmers to be reproduced. Once reproduced, the aim of this project will be to compare the efficiency, power, motion velocity and cost-efficiency of various microrobot designs for mass production of the microswimmers. The fabrication of

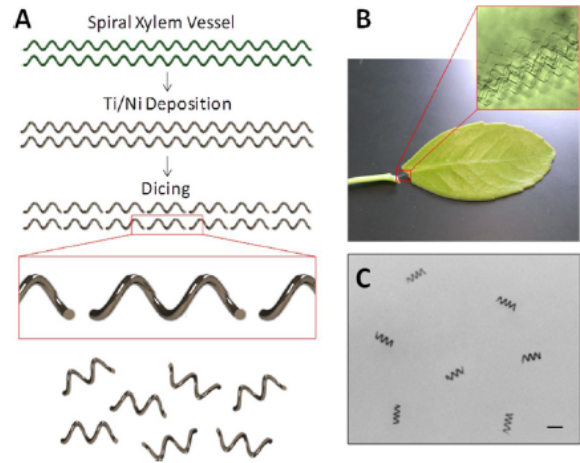


Figure 10: (A) The stages were required to make a plant-based microrobot. (B) A microscopic image of the a xylem helical structure. [2].

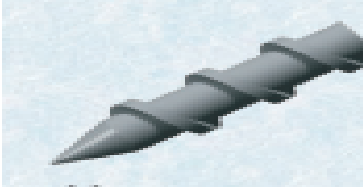

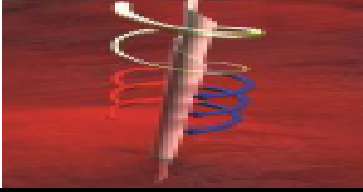
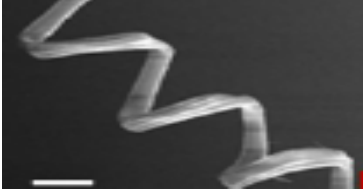

Microrobot Image	Type	Fabrication Method	Citation
	<ul style="list-style-type: none"> • Helical Screw Shape 	<ul style="list-style-type: none"> • Direct Laser Writing (DLW) • Two-photon Polymerization 	<ul style="list-style-type: none"> • [7]
	<ul style="list-style-type: none"> • Flagella Shape 	<ul style="list-style-type: none"> • Direct Laser Writing (DLW) • Two-photon Polymerization 	<ul style="list-style-type: none"> • [8]
	<ul style="list-style-type: none"> • Nanotube 	<ul style="list-style-type: none"> • Molecular Beam Epitaxy (MBE) 	<ul style="list-style-type: none"> • [13]
	<ul style="list-style-type: none"> • Plant-based 	<ul style="list-style-type: none"> • Macerating Plant's Leaves • Seperating Spiral Vessels • Stretching spiral Vessels • Coating with Titanium 	<ul style="list-style-type: none"> • [2]
	<ul style="list-style-type: none"> • Jellyfish 	<ul style="list-style-type: none"> • The EMA coil system 	<ul style="list-style-type: none"> • [4]

Table 1: Different types of microrobots and their fabrication method.

microswimmers will be by Nanoscribe facility using 3D laser lithography. After the microrobots are produced their characteristic will be analysed under the scanning electron microscope in order to identify further improvements in microrobot design.

References

- [1] Eric Diller, Joshua Giltinan, and Metin Sitti. Independent control of multiple magnetic microrobots in three dimensions. *The International Journal of Robotics Research*, 32(5): 614–631, 2013.
- [2] Wei Gao, Xiaomiao Feng, Allen Pei, Christopher R Kane, Ryan Tam, Camille Hennessy,

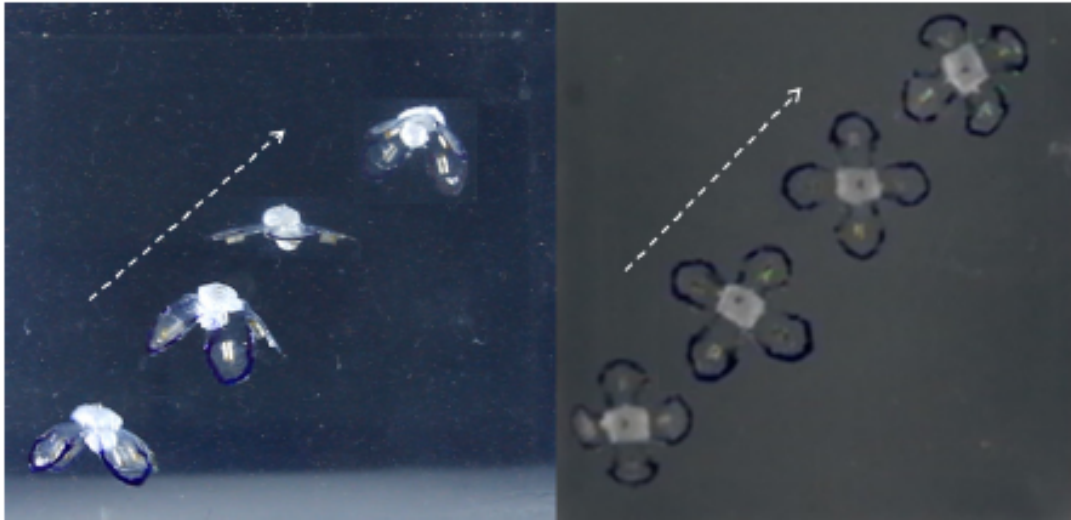


Figure 11: The illustration of microrobot's locomotion from top and side view [4].

and Joseph Wang. Bioinspired helical microswimmers based on vascular plants. *Nano letters*, 14(1):305–310, 2013.

- [3] Sangwon Kim, Famin Qiu, Samhwan Kim, Ali Ghanbari, Cheil Moon, Li Zhang, Bradley J Nelson, and Hongsoo Choi. Fabrication and characterization of magnetic microrobots for three-dimensional cell culture and targeted transportation. *Advanced Materials*, 25(41): 5863–5868, 2013.
- [4] Youngho Ko, Sungyoung Na, Youngwoo Lee, Kyoungrae Cha, Seong Young Ko, Jongoh Park, and Sukho Park. A jellyfish-like swimming mini-robot actuated by an electromagnetic actuation system. *Smart Materials and Structures*, 21(5):057001, 2012.
- [5] Arthur W Mahoney, John C Sarrazin, Eberhard Bamberg, and Jake J Abbott. Velocity control with gravity compensation for magnetic helical microswimmers. *Advanced Robotics*, 25(8):1007–1028, 2011.
- [6] Kathrin E Peyer, Erdem C Siringil, Li Zhang, Marcel Suter, and Bradley J Nelson. Bacteria-inspired magnetic polymer composite microrobots. In *Biomimetic and Biohybrid Systems*, pages 216–227. Springer, 2013.
- [7] Kathrin E Peyer, Soichiro Tottori, Famin Qiu, Li Zhang, and Bradley J Nelson. Magnetic helical micromachines. *Chemistry-A European Journal*, 19(1):28–38, 2013.
- [8] Kathrin E Peyer, Li Zhang, and Bradley J Nelson. Bio-inspired magnetic swimming microrobots for biomedical applications. *Nanoscale*, 5(4):1259–1272, 2013.
- [9] Tian Qiu, John G Gibbs, Debora Schamel, Andrew G Mark, Udit Choudhury, and Peer Fischer. From nanohelices to magnetically actuated microdrills: a universal platform for some of the smallest untethered microrobotic systems for low reynolds number and biological environments.
- [10] Soichiro Tottori and Bradley J Nelson. Artificial helical microswimmers with mastigoneme-inspired appendages. *Biomicrofluidics*, 7(6):061101, 2013.

- [11] Soichiro Tottori, Li Zhang, Famin Qiu, Krzysztof K Krawczyk, Alfredo Franco-Obregón, and Bradley J Nelson. Magnetic helical micromachines: fabrication, controlled swimming, and cargo transport. *Advanced materials*, 24(6):811–816, 2012.
- [12] Dana Vogtmann, Satyandra K Gupta, and Sarah Bergbreiter. Modeling and optimization of a miniature elastomeric compliant mechanism using a 3-spring pseudo rigid body model. In *ASME 2013 International Design Engineering Technical Conferences and Computers and Information in Engineering Conference*, pages V06AT07A036–V06AT07A036. American Society of Mechanical Engineers, 2013.
- [13] Wang Xi, Alexander A. Solovev, Adithya N. Ananth, David H. Gracias, Samuel Sanchez, and Oliver G. Schmidt. Rolled-up magnetic microdrillers: towards remotely controlled minimally invasive surgery. *Nanoscale*, 5:1294–1297, 2013.
- [14] Muhammad A Zeeshan, Roman Grisch, Eva Pellicer, Kartik M Sivaraman, Kathrin E Peyer, Jordi Sort, Berna Özkale, Mahmut S Sakar, Bradley J Nelson, and Salvador Pané. Hybrid helical magnetic microrobots obtained by 3d template-assisted electrodeposition. *Small*, 2013.